Physics and Imaging in Radiation Oncology 8 (2018) 23–27

Contents lists available at ScienceDirect

Physics and Imaging in Radiation Oncology

journal homepage: www.elsevier.com/locate/phro

Original Research Article

The effect of density overrides on magnetic resonance-guided radiation therapy planning for lung cancer

Oliver Schrenk[a,b,c,*], Claudia Katharina Spindeldreier[a,b,d], Daniela Schmitt[a,b,d], Falk Roeder[e,f], Mark Bangert[a,b], Lucas Norberto Burigo[a,b], Asja Pfaffenberger[a,b]

[a] Division of Medical Physics in Radiation Oncology, German Cancer Research Center (DKFZ), Heidelberg, Germany
[b] Heidelberg Institute for Radiation Oncology (HIRO), National Center for Radiation Research in Oncology (NCRO), Heidelberg, Germany
[c] Medical Faculty, University of Heidelberg, Heidelberg, Germany
[d] Department of Radiation Oncology, Heidelberg University Hospital, Heidelberg, Germany
[e] Clinical Cooperation Unit Molecular Radiooncology, German Cancer Research Center (DKFZ), Heidelberg, Germany
[f] Department of Radiation Oncology, University of Munich (LMU), Munich, Germany

ARTICLE INFO

Keywords:
Density overrides
Treatment planning
IMRT
Monte Carlo
MRgRT
MR-linac
Magnetic field
Lung cancer
Dose delivery
Tumor motion

ABSTRACT

Background and Purpose: Inverse treatment planning for lung cancer can be challenging since density heterogeneities may appear inside the planning target volume (PTV). One method to improve the quality of intensity modulation is the override of low density tissues inside the PTV during plan optimization. For magnetic resonance-guided radiation therapy (MRgRT), where the influence of the magnetic field on secondary electrons is sensitive to the tissue density, the reliability of density overrides has not yet been proven. This work, therefore, gains a first insight into density override strategies for MRgRT.

Material and methods: Monte Carlo-based treatment plans for five lung cancer patients were generated based on free-breathing CTs and two density override strategies. Different magnetic field configurations were considered with their effect being accounted for during optimization. Optimized plans were forward calculated to 4D-CTs and accumulated for the comparison of planned and expected delivered dose.

Results: For MRgRT, density overrides led to a discrepancy between the delivered and planned dose. The tumor volume coverage deteriorated for perpendicular magnetic fields of 1.5 T to 93.6% ($D_{98\%}$). For inline fields a maximal increase of 2.2% was found for the mean dose. In terms of organs at risk, a maximal sparing of 0.6 Gy and 0.9 Gy was observed for lung and heart, respectively.

Conclusions: In this work, first results on the effect of density overrides on treatment planning for MRgRT are presented. It was observed that the underestimation of magnetic field effects in overridden densities during treatment planning resulted in an altered delivered dose, depending on the field strength and orientation.

1. Introduction

The implementation of treatment planning margins accounting for the expected position variability of the tumor is one strategy to mitigate motion uncertainties on the dose delivery [1]. For lung cancer, however, an enlarged planning margin will inevitably include low-density tissue into the planning target volume (PTV). This can introduce substantial density heterogeneities to the target volume and presents a difficulty for inverse treatment planning. Particularly, when dose calculations are performed with model-based algorithms capable of accounting accurately for density heterogeneities, high dose gradients can arise inside the PTV [2]. Model-based dose calculation algorithms include physical models to incorporate the effect of heterogeneities on lateral scattering into dose calculation. Typical examples of model-based dose calculation algorithms include kernel superposition, deterministic solution of the linear Boltzmann transport equation or Monte-Carlo methods [3,4].

The aim of conventional intensity-modulated radiotherapy (IMRT) is a conformal, homogenous dose in the PTV. To this end, a higher fluence has to be delivered to low density lung tissues than to tumor tissue with a higher density. Consequently, when performing IMRT, the optimization algorithm will set a higher weight to beamlets superimposing in low density regions inside the PTV. This, however, represents an overprediction of the fluence required to provide sufficient dose to the solid tumor when it is shifted to positions where low density tissue was expected. Furthermore, these strongly weighted beamlets can lead to unnecessarily increased dose to healthy tissue. Wiant et al. could show for an analytic anisotropic algorithm (AAA) that the

* Corresponding author at: Division of Medical Physics in Radiation Oncology, German Cancer Research Center (DKFZ), Heidelberg, Germany.

https://doi.org/10.1016/j.phro.2018.11.003
Received 31 March 2018; Received in revised form 8 November 2018; Accepted 9 November 2018

overriding of CT values inside the PTV for treatment planning improved the dose delivery to the gross tumor volume (GTV) and reduced the dose to surrounding tissues [5].

The presence of a permanent magnetic field in magnetic resonance-guided radiation therapy (MRgRT) influences the dose distribution due to the Lorentz force acting on secondary electrons. The distortion of the dose depends on the orientation and strength of the magnetic field as well as on the patient tissue [6]. Dose effects are known to be particularly strong in lung where high density variations occur [7,8]. These dose effects have to be taken into account during treatment planning and are usually integrated in Monte Carlo-based treatment planning algorithms. The effects of density overrides on the treatment planning for MRgRT have not been evaluated yet. In this work, we investigate the impact of different magnetic field orientations and strength on the dosimetric outcome, when density overrides are applied during IMRT treatment planning for lung cancer patients.

2. Material and methods

2.1. Treatment planning

IMRT step and shoot plans were generated using the in-house developed open-source multimodality treatment planning system matRad [9]. To account for the effect of magnetic field already during optimization, matRad was extended to enable Monte Carlo-based dose calculation using the EGSnrc particle transport code [10]. The particle transport in the presence of magnetic fields was realized by means of a specialized macro integrated into the EGSnrc code [8,11].

The radiation field of a 6 MV linear accelerator was simulated by a simplified fluence-modulated point-source model along with an additional electron point-source to account for contaminating electrons. Single beamlets were set to a 10 x 10 mm^2 cross-section in the isocenter plane. A uniform magnetic field was defined for all simulations, while the impact of the magnetic fringe field was not considered. The maximum electron step-length was set to 0.025 times the gyration radius. The total number of particle histories in the simulations of single beamlets for generation of the dose influence matrix as well as for the forward calculations of the optimized plans was chosen to provide an overall statistical uncertainty of less than 1% for dose in the PTV. An internal target volume (ITV) concept was applied to account for the geometrical uncertainties of the target volume with the ITV defined as the sum of the GTV delineations in all breathing phases of the 4D-CT. For the clinic target volume, a 5 mm margin was added to the ITV. The final PTV encompassed an additional safety margin of 2 mm. For the analysis of the tissue outside the treatment planning volume, a supplementary 5 mm help margin was defined surrounding to the PTV ($MPTV_{+5mm}$).

2.2. Density override strategies

The concept of density overrides was described by Wiant et al. [5]. They introduced various density override strategies and investigated their impact on stereotactic body radiotherapy treatment for lung cancer patients. In their work, four different density override strategies were compared to a free-breathing CT (FBCT) approach, using an AAA for dose calculation. In this work, the two strategies performing best for the AAA in Wiant et al. were selected for the current investigations in the presence of a magnetic field, namely the strategies DO1 and DO2 as described in Fig. 1. Treatment plans were generated for the free-breathing approach, used as a reference condition, and for the two density override strategies. Furthermore, since MRgRT systems enable real-time MR-imaging during irradiation, there is the possibility of margin reduction along with gating or tracking approaches what shall reduce the ratio of lung tissue inside the PTV and eventually mitigate the effect of density overrides. To investigate this issue, a gating PTV was defined as a single 5 mm margin enclosing the GTV. Subsequently,

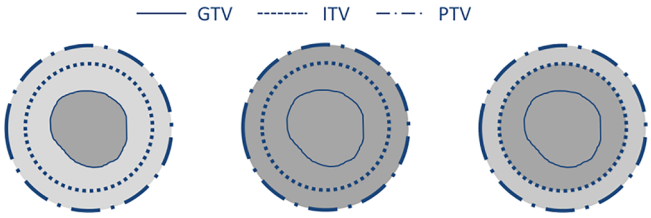

Fig. 1. Schematic representation of the density override strategies adapted from [5]. (left) Free-breathing CT (FBCT). (middle) Density override strategy DO1: the density of the PTV is replaced by the mean density of the GTV. (right) Density override strategy DO2: the density of the ITV is replaced by the mean density of the GTV and the density of the remaining PTV is set to the average density between the mean GTV density and the surrounding tissue described by the mean density of a 5 mm margin surrounding the PTV ($MPTV_{+5mm}$).

Table 1
Table of the density values used for density overrides. (1) Mean density $\bar{\rho}$ of the GTV; (2) mean density $\bar{\rho}$ of the $MPTV_{+5mm}$; (3) average of (1) and (2). All values are listed in g/cm^3.

	Pat A_{DO}	Pat B_{DO}	Pat C_{DO}	Pat D_{DO}	Pat E_{DO}
(1) $\bar{\rho}$ (GTV)	0.75	0.76	0.90	0.98	0.90
(2) $\bar{\rho}$ ($MPTV_{+5mm}$)	0.37	0.52	0.52	0.80	0.43
(3) Av. of (1) & (2)	0.56	0.64	0.71	0.89	0.88

the density override concept DO1 was applied on the gating PTV for treatment planning ($DO1_{gating}$).

The mean density values used to override the density of the voxels inside the ITV and the PTV are listed in table 1, for the patient data set investigated in this work. In addition, Fig. 2 shows the distribution of density values inside the GTV and $MPTV_{+5mm}$.

2.3. Study design

IMRT plans were created for five lung cancer patients considering two different magnetic field to beam orientations each with two different magnetic field strengths as described in the literature, namely a 0.35 T and 1.5 T magnetic field perpendicular to the beam direction, and a 0.5 T and 1.0 T inline magnetic [12–15]. Optimization was performed according to the RTOG 1021 guideline [16] with the optimization goal of homogeneous dose in the PTV within $D_{98\%} > 95\%$ and D_2 less than 107% of prescribed dose. Further details about the treatment planning set-up for individual patients are listed in table 2.

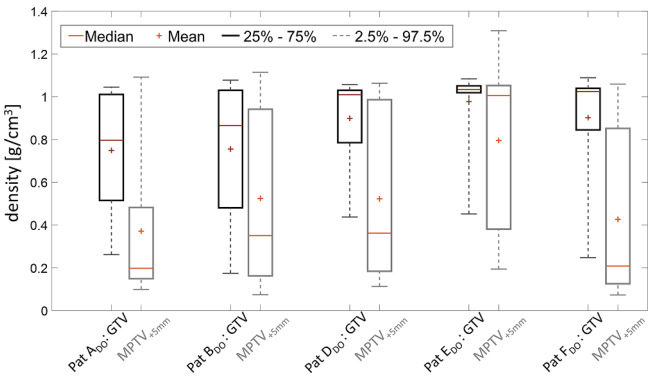

Fig. 2. Boxplot distribution of the density values inside the GTV (black) and $MPTV_{+5mm}$ (grey).

Table 2
Overview of patient-specific data used in this study. $DO1_{gating}$ refers to a gating margin of 5 mm added to the GTV.

Patient	Tumor location	No. of Beams	Volume [cm³]			Volume [cm³]
			GTV	PTV	$DO1_{gating}$	Ipsilateral lung
A	Right Upper Lobe	9	10.6	47.1	45.3	1575.7
B	Left Upper Lobe	10	27.0	102.8	90.7	2650.0
C	Right Middle Lobe	10	50.3	169.2	145.5	2086.6
D	Left Upper Lobe	10	91.6	166.2	217.8	1551.3
E	Right Middle Lobe	10	47.0	138.6	157.2	2142.3

After optimization, plans were forward calculated to the corresponding 4D-CT phases without density overrides. The total dose of all ten breathing phases was then accumulated to the initial FBCT using deformable B-spline-based image registration with plastimatch [17] and dose accumulation based on energy mass transformation [18]. In this way, the planned dose with density overrides could be compared to the expected delivered dose. The current analysis was based on imaging data from patients enrolled in a prospective multicenter trial (NCT01396551) investigating real-time lung tumor motion monitoring based on implanted anchored electromagnetic transponders. The trial was approved by the independent ethics committee of the College of Heidelberg (MZmu-026/2011).

3. Results

3.1. Dose evaluation in the tumor

To evaluate the robustness of the dose delivery when density overrides are performed, the planned dose on free-breathing CTs with density overrides was compared to the forward-calculated dose on 4D-CT data without density overrides, representing the expected delivered dose. Fig. 3 shows the mean dose metrics of $D_{98\%}$, D_{mean} and $D_{2\%}$ in the GTV for all patients. All plans showed comparable dose quality for the case of FBCTs where no density override was applied. Independent of the magnetic field present the difference between planned dose and delivered dose to the GTV was less than 0.4%. However, when density overrides were applied during optimization, the planned dose and delivered dose differed substantially in the presence of magnetic fields, with the effect depending on the magnetic field strength and orientation.

For the case of perpendicular magnetic fields, the gap between $D_{98\%}$ and $D_{2\%}$ of the forward-calculated plans increased, leading to a considerable deterioration of the dose conformity in the GTV. This effect increased with the higher magnetic field strength. In the perpendicular magnetic field of 0.35 T, $D_{98\%}$ was reduced to 95.4% and 95.6% of the prescribed dose for DO1 and DO2, respectively, while $D_{2\%}$ raised to 104.6% and 104.1%. The 1.5 T perpendicular magnetic field resulted in average $D_{98\%}$ values of 93.6% and 94.0% for DO1 and DO2, respectively, and average $D_{2\%}$ values of 107.1% and 106.8%. D_{mean} did not change substantially due to the presence of perpendicular magnetic fields.

The presence of inline magnetic fields resulted in an overall increase of delivered dose to the GTV in comparison to the planned dose. For the inline magnetic field of 0.5 T, the average D_{mean} increased by 1.5% for DO1 and 1.3% for DO2. As for the case of a 1.0 T inline magnetic field, D_{mean} increased by 2.2% and 1.9% for DO1 and DO2, respectively. In addition, the average $D_{98\%}$ and $D_{2\%}$ values were also enhanced by the presence of inline magnetic fields.

The results of the simulations for the case of $DO1_{gating}$, showed no relevant deviations to DO1 with the conventional PTV margins.

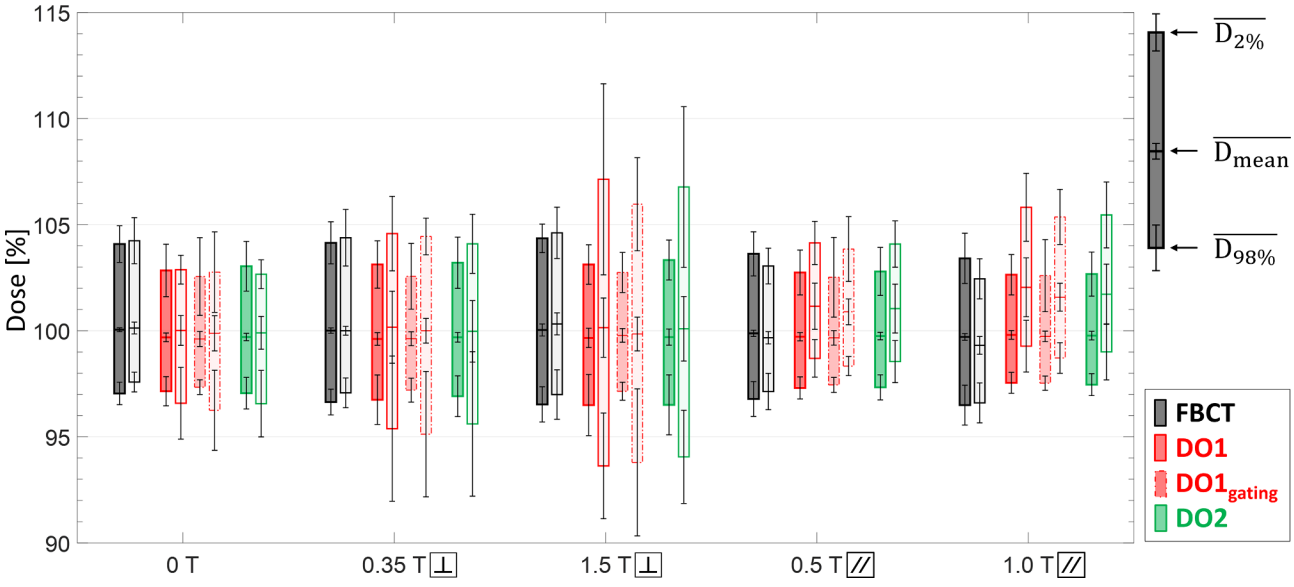

Fig. 3. Average values across the five lung cancer patients for the GTV dose metrics of $D_{2\%}$, D_{mean} and $D_{98\%}$. The prescribed dose is here represented with 100%. Error bars indicate corresponding standard deviations. Bars with black outline depict results from FBCT, dark red from DO1 and green from DO2 approaches. The results from treatment planning based on a reduced gating margin are represented by bars with red dashed-dotted outline ($DO1_{gating}$). Dark-colored bars present the results from treatment plan optimization taking into account the magnetic field during optimization, while light-colored bars present dose metrics for the forward-calculated dose to 4D-CT phases accumulated to the corresponding free-breathing CT. (For interpretation of the references to colour in this figure legend, the reader is referred to the web version of this article.)

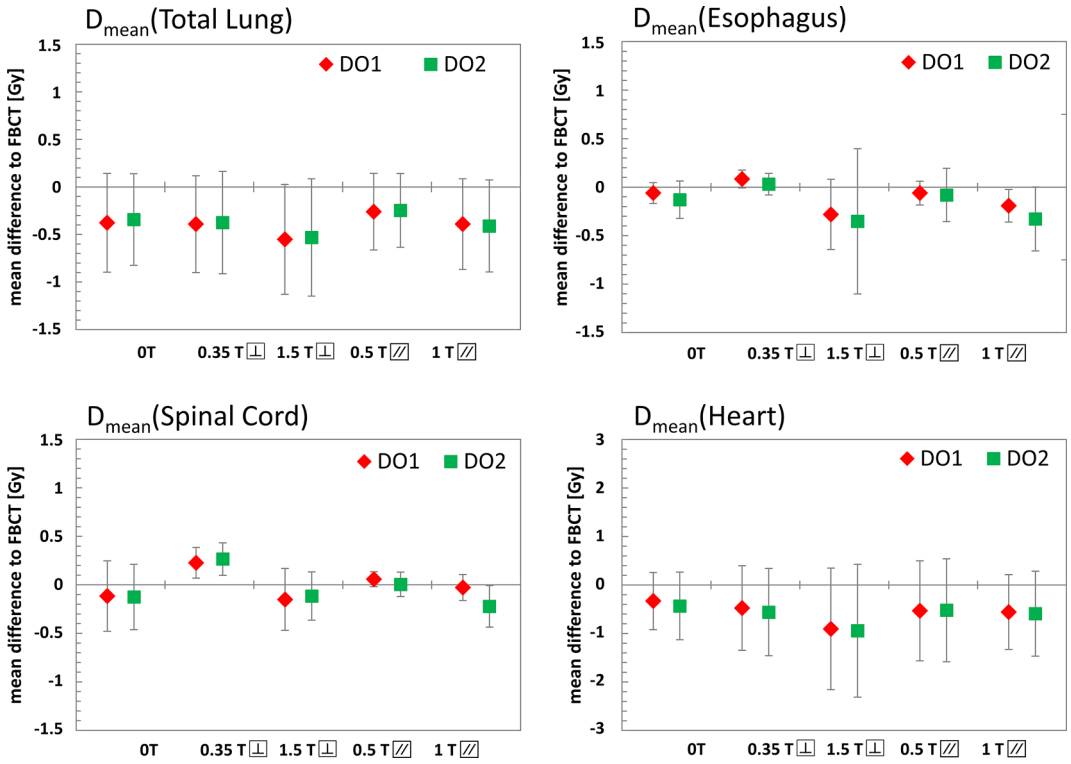

Fig. 4. Differences between the FBCT strategy and the density override strategies DO1 and DO2 in terms of mean dose (D_{mean}) to organs at risk, including the total lung, esophagus, spinal cord, and heart. The mean difference is calculated over all patients. All values stated are in absolute dose assuming a prescribed dose of 70 Gy.

3.2. Dose evaluation at OAR

The differences between the conventional FBCT strategy and the density override strategies DO1 and DO2 in terms of dose to organs at risk are shown in Fig. 4. The results showed neither clear general dependency on the magnetic field strength or orientation, nor on the density override strategy itself.

For the dose to the total lung, the average D_{mean} was reduced in all cases. A minimal D_{mean} reduction of 0.3 Gy for DO1 and 0.2 Gy for DO2 was found for the 0.5 T inline magnetic fields, while a maximal reduction of 0.6 Gy for DO1 and 0.5 Gy for DO2 was observed for the case of a 1.5 T perpendicular magnetic field.

The average mean doses to the esophagus and spinal cord did not show any pronounced tendencies. The mean esophagus dose decreases for 0 T, 1.5 T perpendicular, 0.5 T and 1.0 T inline magnetic fields by a maximum of 0.3 Gy, while it increased slightly by 0.1 Gy for DO1 in a 0.35 T perpendicular magnetic field. The mean dose to the spinal cord was reduced for 0 T, 1.5 T perpendicular and 1.0 T inline magnetic fields by less than 0.2 Gy while it increased for the 0.35 T perpendicular and 0.5 T inline magnetic fields by maximal 0.3 Gy. The largest dose reduction gained by density overrides was observed in the heart where the average D_{mean} decreased by up to 0.9 Gy for DO1 and DO2 in a 1.5 T perpendicular magnetic field.

4. Discussion

The strategy of density overrides for lung cancer radiation treatment planning can be advantageous for conventional IMRT. The assumption of a homogeneous density inside the PTV, equal to the density of the solid tumor, allows the optimization algorithm to generate a superior fluence modulation with optimal dose coverage, independent of the solid tumor location inside the PTV. For MRgRT, the impact of the magnetic field on the dose distribution depends on the field strength and orientation as well as on the density of the tissue in which secondary electrons propagate. This study provides an insight into the effects of density override strategies on lung cancer treatment planning for different magnetic field set-ups.

For conventional IMRT treatment planning, Wiant et al. could demonstrate that density override strategies are beneficial for the treatment plan quality of lung cancer patients [5]. Moreover, an improved stability of dose distributions in lung was reported during organ motion, when a homogeneous density override was applied with a density of 1 g/cm^3 [2,19]. In this work, similar results related to conventional radiotherapy were obtained. In terms of dose to organs at risk, density overrides were observed to improve the healthy tissue sparing, with the mean dose being reduced when no magnetic field is present. These results are in agreement with Wiant et al., where planned and delivered dose only differed slightly. Furthermore, the impact of considered magnetic fields on the FBCT approach was investigated and no substantial differences were observed between the planned and accumulated delivered dose. Treatment planning strategies using CT data acquired from dynamic or temporal information of 4D-CTs such as maximal- or average- intensity projection as well as breath-holding techniques were not incorporated in this work [20–22].

When treatment planning was performed in the presence of magnetic fields and density override strategies were applied, the results for the delivered dose differed substantially from the planned dose. For the considered perpendicular magnetic fields, results showed a loss of dose conformity in the GTV due to underestimation of the electron return effect in regions where low-density tissues were replaced during treatment planning. This impact was more pronounced for the magnetic field of 1.5 T than for 0.35 T. For the 1.5 T perpendicular magnetic field, results indicated that a considerable part of the GTV received less than 95% of the prescribed dose. An underdosage of this extend may compromise tumor control and counterbalance the possible benefits of MRgRT.

Inline oriented magnetic fields caused a reduction of laterally scattered electrons and led to a pronounced forward orientation of secondary electrons. This effect was underestimated when density override strategies were applied for treatment planning and eventually

resulted in an increased delivered dose to the GTV. The dose increase in the GTV was more pronounced for the inline magnetic field of 1.0 T than for 0.5 T. The effect of the inline magnetic fields on dose values, however, was small and it is not expected to have a substantial impact on the treatment outcome.

For the two investigated density override strategies DO1 and DO2, no significant differences were found, indicating an equivalence of both strategies. In terms of dose to OARs, the results showed neither clear dependency on the magnetic field orientation and strength nor on the density override strategy itself. A systematic decrease in D_{mean} was only found for the heart and total lung. The dose sparing, however, was small and did not exceed 1 Gy.

The results presented in this work provide a first insight into the effect of density overrides on treatment planning for MRgRT. It could be shown that the underestimation of the impact of magnetic fields on secondary electrons in overridden densities during treatment planning can limit the applicability of density override strategies for MRgRT. While for inline magnetic fields the effects are only small, density overrides can lead to systematical underdosage of the tumor for perpendicular magnetic fields of 1.5 T. More conformal results were obtained when the FBCT was used for treatment planning. From the cases studied the conclusion can be drawn that for MRgRT a recalculation of optimized plans on the original CT is mandatory when density override strategies are applied during treatment planning. The suitability of density overrides, particularly for perpendicular magnetic fields, needs to be determined case-specific.

Conflict of interest

The authors declare to have no conflict of interest.

References

[1] Allisy A, Wambersie A. ICRU Report 62 - Prescribing, Recording, and Reporting Photon Beam Therapy (Supplement to ICRU Report 50). J Int Comm Radiat Units Meas 1999(1):55. https://doi.org/10.1259/bjr.74.879.740294.

[2] Edmunds K, Bedford J. Assessment of the robustness of volumetricmodulated arc therapy for lung radiotherapy. Br J Radiol 2013;86(1023). https://doi.org/10.1259/bjr.20120498.

[3] Oelkfe U, Scholz C. Schlegel W, Bortfeld T, Grosu A-.L, editors. Algorithms New Technologies in Radiation Oncology Berlin Heidelberg: Springer; 2006. p. 187–96. https://doi.org/10.1007/3-540-29999-8_15.

[4] Sloboda RS, Morrison H, Cawston-Grant B, Menon GV. A brief look at model-based dose calculation principles, practicalities, and promise. J Contemp Brachyther 2017;9(1):79–88. https://doi.org/10.5114/jcb.2017.65849.

[5] Wiant D, Vanderstraeten C, Maurer J, Pursley J, Terrell J, Sintay BJ. On the validity of density overrides for VMAT lung SBRT planning. Med Phys 2014;41(8):81707. https://doi.org/10.1118/1.4887778.

[6] Raaijmakers aJE, Hårdemark B, Raaymakers BW, Raaijmakers CPJ, Lagendijk JJW. Dose optimization for the MRI-accelerator: IMRT in the presence of a magnetic field. Phys Med Biol 2007;52(23):7045–54. https://doi.org/10.1088/0031-9155/52/23/018.

[7] Kirkby C, Murray B, Rathee S, Fallone BG. Lung dosimetry in a linac-MRI radiotherapy unit with a longitudinal magnetic field. Med Phys 2010;37(9):4722–32. https://doi.org/10.1118/1.3475942.

[8] Schrenk O, Spindeldreier CK, Burigo LN, Hoerner-Rieber J, Pfaffenberger A. Effects of magnetic field orientation and strength on the treatment planning of non-small cell lung cancer. Med Phys 2017;44(12):6621–31. https://doi.org/10.1002/mp.12631.

[9] Wieser HP, et al. Development of the open-source dose calculation and optimization toolkit matRad. Med Phys 2017;44(6):2556–68. https://doi.org/10.1002/mp.12251.

[10] Kawrakow I, Mainegra-Hing E, Rogers DWO, Tessier F, Walters BRB. The EGSnrc Code System: Monte Carlo Simulation of Electron and Photon Transport," Ottawa, Canada; 2015.

[11] Spindeldreier CK, et al. Radiation dosimetry in magnetic fields with Farmer-type ionization chambers: Determination of magnetic field correction factors for different magnetic field strengths and field orientations. Phys Med Biol 2017;62(16):6708–28. https://doi.org/10.1088/1361-6560/aa7ae4.

[12] Mutic S, Dempsey JF. The viewray system: magnetic resonance-guided and controlled radiotherapy. Semin Radiat Oncol 2014;24(3):196–9. https://doi.org/10.1016/j.semradonc.2014.02.008.

[13] Fallone BG. The rotating biplanar linac-magnetic resonance imaging system. Semin Radiat Oncol 2014;24(3):200–2. https://doi.org/10.1016/j.semradonc.2014.02.011.

[14] Keall PJ, Barton M, Crozier S. The australian magnetic resonance imaging-linac program. Semin Radiat Oncol 2014;24(3):203–6. https://doi.org/10.1016/j.semradonc.2014.02.015.

[15] Lagendijk JJW, Raaymakers BW, van Vulpen M. The magnetic resonance imaging-linac system. Semin Radiat Oncol 2014;24(3):207–9. https://doi.org/10.1016/j.semradonc.2014.02.009.

[16] RTOG Foundation, "RTOG 1021 – A Randomized Phase III Study of Sublobar Resection (± Brachytherapy) versus Stereotactic Body Radiation Therapy in High Risk Patients with Stage I Non-Small Cell Lung Cancer (NSCLC)", Timmerman, Robert Online Available: https://www.rtog.org/ClinicalTrials/ProtocolTable/StudyDetails.aspx?study=1021 2013 (accessed: 05.05.17.).

[17] Sharp G, et al. Plastimatch: an open source software suite for radiotherapy image processing. Proc XVI'th Int Conf use Comput Radiother 2010;2017.

[18] Li HS, et al. Direct dose mapping versus energy/mass transfer mapping for 4D dose accumulation: fundamental differences and dosimetric consequences. Phys Med Biol 2014;59:173–88. https://doi.org/10.1088/0031-9155/59/1/173.

[19] Ehler ED, Tome WA, Lung 4D-IMRT treatment planning: An evaluation of three methods applied to four-dimensional data sets. vol. 88, pp. 319–325, 2008. https://doi.org/10.1016/j.radonc.2008.07.004.

[20] Benedict SH, et al. Stereotactic body radiation therapy: the report of AAPM task group 101. Med Phys 2010;37(8):4078–101. https://doi.org/10.1118/1.3438081.

[21] Tian Z, Folkerts M, Li Y, Shi F, Jiang SB, Jia X, An Analytic Linear Accelerator Source Model for Monte Carlo dose calculations. II. Model Utilization in a GPU – based Monte Carlo Package and Automatic Source Commissioning, pp. 1–19, 2015. https://doi.org/10.1118/1.4705353.

[22] Hanley J, et al. Deep inspiration breath-hold technique for lung tumors: The potential value of target immobilization and reduced lung density in dose escalation. Int J Radiat Oncol Biol Phys 1999;45(3):603–11. https://doi.org/10.1016/S0360-3016(99)00154-6.